Accepted Manuscript

Studies on the thermal stability of $BiFeO_3$ and the phase diagram of Bi-Fe-O system

A.V. Meera, Rajesh Ganesan, T. Gnanasekaran

PII: S0925-8388(19)31021-7

DOI: https://doi.org/10.1016/j.jallcom.2019.03.205

Reference: JALCOM 49969

To appear in: *Journal of Alloys and Compounds*

Received Date: 4 January 2019

Revised Date: 9 March 2019

Accepted Date: 13 March 2019

Please cite this article as: A.V. Meera, R. Ganesan, T. Gnanasekaran, Studies on the thermal stability of $BiFeO_3$ and the phase diagram of Bi-Fe-O system, *Journal of Alloys and Compounds* (2019), doi: https://doi.org/10.1016/j.jallcom.2019.03.205.

This is a PDF file of an unedited manuscript that has been accepted for publication. As a service to our customers we are providing this early version of the manuscript. The manuscript will undergo copyediting, typesetting, and review of the resulting proof before it is published in its final form. Please note that during the production process errors may be discovered which could affect the content, and all legal disclaimers that apply to the journal pertain.

ACCEPTED MANUSCRIPT

Studies on the thermal stability of $BiFeO_3$ and the phase diagram of Bi-Fe-O system

A.V. Meera, Rajesh Ganesan* and T.Gnanasekaran

Materials Chemistry Division, Materials Chemistry and Metal Fuel Cycle Group

Indira Gandhi Centre for Atomic Research, HBNI, Kalpakkam 603 102, India

*Corresponding Author:

Dr. Rajesh Ganesan

Indira Gandhi Centre for Atomic Research

Kalpakkam 603 102, India

Email: rajesh@igcar.gov.in

Abstract

The thermal stability of $BiFeO_3$ was examined by different experimental techniques and found that it is metastable at low temperatures and it attains thermodynamic stability at around 940 K. Long term equilibration studies at 773 and 1023 K, and characterization of coexisting phases by XRD revealed the phase fields. Based on this, the isothermal section of the ternary phase diagram of Bi-Fe-O system was constructed at 773 and 1023 K.

Key words: Coolant, Bi-Fe-O system, Equilibration, Phase diagram, Thermal stability, Emf measurement.

1. Introduction

Liquid lead and lead-bismuth eutectic alloy are considered as candidate coolant and spallation target in Accelerator Driven Systems (ADS). They are also considered as candidate coolants in advanced nuclear reactors. However, they are highly corrosive towards

the structural steels, and this is because of the high solubility of the major alloying elements in them [1]. This corrosion could be minimized by forming a passive oxide layer on the steels by maintaining controlled oxygen levels in the liquid metal coolant [2]. To understand the composition and thermodynamic stability of the passive oxide film, information on the phase diagrams of Pb-M-O and Bi-M-O (M = alloying elements in steels) systems as well as the thermodynamic data of the relevant ternary compounds existing in these systems are required. Our studies on Pb-Fe-O and Pb-Cr-O systems were earlier reported [3-8]. A partial phase diagram of Bi-Fe-O system and the standard Gibbs energy of formation of one of the ternary compounds of this system viz., $Bi_2Fe_4O_9$ have been reported by the present authors recently [9]. This paper presents the results of the studies carried out to establish the thermal stability of $BiFeO_3$ and the investigations to deduce the complete phase diagram of Bi-Fe-O system at 773 and 1023 K.

2. Literature Survey

Pseudo-binary Bi_2O_3-Fe_2O_3 system was investigated by several authors in the past [10-19]. Salient features of these investigations were in reference 9. In Bi-Fe-O system, only three ternary compounds viz., $Bi_{25}FeO_{39}$, $Bi_2Fe_4O_9$ and $BiFeO_3$ are present. Phapale et al. [20] measured the thermochemical properties of these compounds by calorimetry. They measured enthalpy of formation ($\Delta H°_{f,298\ K}$) of these compounds by acid solution calorimetry and molar heat capacity by differential scanning calorimetry. Using the data, they deduced their Gibbs energy of formation using estimated values for the entropy of formation. $BiFeO_3$ is one of the most widely studied multiferroic material and a candidate for new generation of lead-free electroceramics [21-23]. Zhang et al. [21] reviewed on chemical-route derived nanostructured $BiFeO_3$ such as thin films, nanowires, and nanoparticles. Wu et al.[22] discussed about the $BiFeO_3$ based ceramic bulk, thin films, and

nanostructures of $BiFeO_3$ and their multifunctional applications. Synthesis and characterization of electrical features of $BiFeO_3$ and the effect of doping were reviewed by Molak et al. [23]. Experimentally determined temperature range of stability of $BiFeO_3$ reported by different authors is not in agreement. Attempts by Achenbach et al. [24] to prepare phase pure $BiFeO_3$ by solid-state reaction between Bi_2O_3 and Fe_2O_3 at temperatures below 973 K were unsuccessful, and they observed the reaction to be incomplete. They also reported $BiFeO_3$ to be unstable above 1023 K. According to them, the formation of $Bi_2Fe_4O_9$ was energetically competitive to the formation of $BiFeO_3$ in the temperature range of 973 to 1023 K. Preparation of $BiFeO_3$ always yielded a small amount of $Bi_2Fe_4O_9$ and the corresponding amount of residual Bi_2O_3. They could prepare phase pure $BiFeO_3$ only by taking an excess of Bi_2O_3 (Bi_2O_3:Fe_2O_3 = 2:1) and heating in the air at 1023 K followed by air quenching and removal of the excess Bi_2O_3 by leaching with concentrated HNO_3. Experiments by De Sitter et al. [25] confirmed these observations. Morozov et al. [26] studied the characteristics of formation of $BiFeO_3$ and concluded that $BiFeO_3$ prepared by heating a mixture of Bi_2O_3 and Fe_2O_3 always contained impurity phases such as the phase with γ-Bi_2O_3 structure and $Bi_2Fe_4O_9$, presumably due to slow kinetics. Valant et al. [27] reported that phase pure $BiFeO_3$ could be prepared by heating together high purity (99.9995 % pure) iron and bismuth oxides. They showed that the presence of impurities of the order of 0.1 mol% in the reactants could produce ~3 vol% $Bi_{25}FeO_{39}$ and 7.6 vol% of $Bi_2Fe_4O_9$. Carvalho and Tavares [28] reported that temperature and time were critical in the synthesis of phase pure $BiFeO_3$. According to them, higher $BiFeO_3$ content could be obtained by a thermal treatment at 873 K for 1 h. Preparations at temperatures below and above this temperature always yielded secondary phases, namely, $Bi_2Fe_4O_9$ and $Bi_{25}FeO_{39}$. Also, heat treatment for a longer time at 873 K resulted in the decomposition of $BiFeO_3$ to the secondary phases. So they concluded that $BiFeO_3$ to be metastable at 873 K [28]. Selbach et

al. [29] studied the thermodynamic stability of $BiFeO_3$. High-temperature XRD (HTXRD) experiments performed on $BiFeO_3$ prepared by solid-state route as well as by wet chemical route and the analysis of the isothermally heat-treated Bi_2O_3-Fe_2O_3 mixtures, showed that $BiFeO_3$ was metastable in the temperature range of 720 to 1040 K and decomposed to give $Bi_2Fe_4O_9$ and $Bi_{25}FeO_{39}$. At higher temperatures, these secondary phases reacted back to form $BiFeO_3$. Using thermodynamic data reported by Phapale et al. [20], they deduced the standard Gibbs energy change of the following reaction to be positive in the temperature range of 720 to 1040 K and would be negative above 1040 K indicating $BiFeO_3$ to be stable only above 1040 K:

$$Bi_{25}FeO_{39} + 12\ Bi_2Fe_4O_9 \rightarrow 49\ BiFeO_3$$

Lu et al. [19], based on their studies using 99.999 wt% Bi_2O_3 and 99.99 wt% Fe_2O_3, determined the peritectic decomposition temperature of $BiFeO_3$ as 1125 K and identified a ferroelectric transition for this compound at 1098 K. Maurya et al. [30] studied the reactions in equimolar mixtures of Bi_2O_3 and Fe_2O_3 by heating them at different temperatures for 1 h in the air and recording the XRD patterns of the products after cooling them to room temperature. The authors found that $Bi_{25}FeO_{39}$ (the authors represented it as $Bi_{25}FeO_{40}$) was formed at temperatures above 823 K followed by the appearance of $BiFeO_3$ phase at 973 K. The impurity phase viz., $Bi_{25}FeO_{39}$ was present at all those temperatures. Activation of the reactants by ball milling reduced the temperatures by about 100 K but the results obtained were similar. Egorysheva et al. [31] investigated the extent of formation of $BiFeO_3$ when equimolar mixtures of Bi_2O_3 and Fe_2O_3 were heated in the air for 20 minutes at 873 K, 973 K, 1023 K, 1073 K, and 1123 K. Their experiments showed that $BiFeO_3$ did not form at 873 K while $Bi_{25}FeO_{39}$ was formed as major phase. From 973 K onwards $BiFeO_3$ was one of the phases formed, and its fraction gradually increased with increase in temperature. At 1123 K, $BiFeO_3$ was the major phase while $Bi_{25}FeO_{39}$ was present as a minor phase. The authors

reasoned that $Bi_{25}FeO_{39}$ was formed (during the initial phase of the reaction) in large fraction because of its wide homogeneity range and high diffusion coefficient of Bi^{3+} in it, in comparison with the corresponding diffusion coefficients in $BiFeO_3$, Bi_2O_3, and Fe_2O_3. The diffusion coefficient of Bi^{3+} in $Bi_{25}FeO_{39}$ at 1013 K was reported as 1.5×10^{-8} m^2 s^{-1} while in $BiFeO_3$ it was reported as 3.2×10^{-16} m^2 s^{-1}. The corresponding reported values in Bi_2O_3 and Fe_2O_3 were found to be 1.3×10^{-17} m^2 s^{-1}. Lomanova and Gusarov [32] studied the reactions between coprecipitated bismuth and iron hydroxides while heating them in a stepwise manner with isothermal equilibrations at 753, 773, 793, 813, 833, 873 and 903 K for 5 to 7 minutes followed by high-temperature XRD measurements. Their results showed $BiFeO_3$ and $Bi_{25}FeO_{39}$ form at 753 K. At 773 and 793 K, $Bi_2Fe_4O_9$ appeared along with $BiFeO_3$ and $Bi_{25}FeO_{39}$. At 813 K and above, the fraction of $Bi_2Fe_4O_9$ increased while that of $Bi_{25}FeO_{39}$ decreased substantially.

To summarize, the thermodynamic stability of $BiFeO_3$ has been under disagreement. Even preparation of phase pure $BiFeO_3$ was difficult which was attributed to the purity of chemicals used. Even though a partial phase diagram of Bi-Fe-O system was established in the author's laboratory, a complete phase diagram of Bi-Fe-O ternary system was not deduced.

3. Experimental

Bi_2O_3 powder (99.99 wt% purity on metals basis, M/s Alfa Aesar, UK), Fe_2O_3 powder (99.99 wt% purity on metals basis, M/s Alfa Aesar, UK) were used as the starting materials for the preparation of the ternary compounds. For phase equilibration studies, Fe powder (99.9+ wt% purity on metals basis, M/s Alfa Aesar, USA), FeO (99.9 wt%, M/s Cerac, USA) and Bi powder (99.5 wt% on metals basis, M/s Alfa Aesar, USA) were also used as the starting materials. Fe_3O_4 was prepared by reducing Fe_2O_3 at 800 K for 6 h under

Ar-1% hydrogen gas mixture saturated with water vapor. Bi_2O_3 was calcined in the air at 973 K for 5 h to remove the carbonate impurity and moisture while Fe_2O_3 was calcined at 523 K for 2 h to remove the moisture. These oxides were stored in a desiccator before using them in experiments.

3.1 Preparation of ternary oxides:

The ternary compounds were prepared by solid-state reaction between Bi_2O_3 and Fe_2O_3 taken in appropriate molar ratios. The starting materials were ground thoroughly, made in the form of pellets and heated in platinum crucibles for 144 h in the air at 973 K for preparing $Bi_{25}FeO_{39}$ and $Bi_2Fe_4O_9$. For preparing $BiFeO_3$, the temperature chosen was 1073 K. All these samples were ground at the end of 50% of the total time of heating. They were repelletized followed by heating at the same temperature. The resulting products were characterized by XRD. $BiFeO_3$ and $Bi_2Fe_4O_9$ were also prepared by a method involving co-precipitation of the hydroxides. For this preparation, stoichiometric amounts of Bi_2O_3 and Fe_2O_3 were first dissolved in a minimum amount of hot nitric acid (35.2 mol kg^{-1}), and the resultant nitrate solution was added to an excess ammonium hydroxide solution. The precipitate formed was then filtered, washed, dried, and heated in the air at 773 K for 24 h while preparing $BiFeO_3$. While preparing $Bi_2Fe_4O_9$, the temperature of heating was 823 K in the air. The products obtained were characterized by XRD. Phase purity and compositional homogeneity were checked by SEM/EDS. The prepared compounds assayed for the metallic impurities present in them by using inductively coupled plasma atomic emission spectroscopy (ICP-AES). Bi to Fe ratio in the prepared samples was also determined by ICP-AES.

3.2. Investigations on thermal stability of $BiFeO_3$

To determine the temperature range of stability of $BiFeO_3$, studies involving thermogravimetry/differential thermal analysis (TG/DTA), differential scanning calorimetry (DSC), long term equilibrations and oxygen potential measurements were carried out.

3.2.1. TG/DTA and DSC studies with $BiFeO_3$

For the TG/DTA experiment, ~50 mg of $BiFeO_3$ taken in Pt crucible was heated up to 973 K in argon atmosphere at a heating rate of 10 K/min followed by cooling at a rate of 10 K/min up to room temperature, and the thermal events were analyzed using TG/DTA system, SETSYS Evolution 16/18 model, M/s Setaram, France. After the experiment, the sample was characterized by XRD for identifying any change it might have undergone during TG/DTA experiments. Thermal behavior of $BiFeO_3$ was also studied by DSC. Approximately 150 mg of sample was used, and DSC runs were carried out up to 823 K at a heating rate of 10 K/min in an argon atmosphere and maintained at that temperature for 10 minutes. The sample was then cooled to room temperature. A heat-flux type differential scanning calorimeter, of M/s. Mettler Toledo GmbH (model number DSC821e/700), Switzerland was used in this study. Before and after the experiment, the sample was characterized by XRD.

3.2.2. Equilibration of $BiFeO_3$ in the vacuum and the air at different temperatures

As discussed in section 2, $BiFeO_3$ has been reported to be metastable at low temperatures (720 to 1040 K) and attains thermodynamic stability at relatively high-temperature (above 1040 K). Hence, experiments involving equilibrating $BiFeO_3$ in the air and vacuum for prolonged periods were carried out to determine the temperature range of stability of this compound. The schematic of the experimental setup used for this study is shown in Fig. 1. For this experiment, $BiFeO_3$ prepared by co-precipitation method described in section 3.1 was used. Samples made in the form of pellets were taken in zirconia

crucibles. Crucibles containing the pellets were placed in two one-end closed quartz tubes (45 cm long and 1.5 cm dia) at different heights using quartz spacers. In each quartz tube, nine samples were loaded. One of the quartz tubes was sealed under vacuum (10^{-6} torr) while the other tube was kept open to air. A K-type thermocouple which can move vertically at a low speed (0.38 cm/min) with the help of a motor was inserted inside another quartz tube of 8 mm diameter and was used to measure the temperature of the samples as a function of its height. The three quartz tubes were tied together and placed inside a temperature gradient furnace assembly. The assembly consisted of two furnaces which were stacked one over the other. The temperature of each furnace was maintained at different temperatures and controlled within ± 1 K. This arrangement was useful to maintain a required temperature gradient in the furnace. The temperature data was logged using a data acquisition system. From the actual position of the sample, the temperatures of the samples were determined. The temperature of the samples varied between 716 to 1121 K. Samples were equilibrated for 480 h, quenched in ice-cold water and the products were characterized by XRD. The details of the equilibrations are given in Tables 1 and 2.

3.2.3. Equilibration of samples containing $BiFeO_3$ with liquid Bi

Thermal stability of $BiFeO_3$ was also examined by equilibrating phase mixtures containing $BiFeO_3$ with liquid Bi. Equilibrations were carried out at 873, and 1023 K. Starting materials were made in the form of porous pellets. They were kept forcibly immersed in liquid Bi (taken in alumina crucibles) using alumina strips tied to the crucible as the density of pellets are less than that of liquid Bi. The sample preparation was carried out in an inert atmosphere glove box. Then the samples were taken out from the glove box, vacuum sealed in quartz ampoules and equilibrated at the chosen temperatures for 480 h.

After equilibration, the ampoules were quenched in ice-cold water; the samples were retrieved and characterized by XRD. The details of these equilibrations are given in Table 3.

3.3 Additional phase equilibrations

To determine the phase fields in the ternary Bi-Fe-O system, equilibrations were carried out by taking appropriate mixtures of bismuth and iron metal powders and their oxides. After thorough mixing, the starting materials were made into pellets. The pellets were placed in zirconia crucibles which were hermetically sealed inside copper tubes. The sealing was carried out by pulsed tungsten inert gas welding inside an argon atmosphere glove box containing < 5 ppm of oxygen and moisture. The samples in copper tubes were then equilibrated by placing them in a stainless steel vessel under flowing argon gas. The temperature and total duration of equilibrations were 1023 K and 480 h, respectively. All the equilibrations were carried out with one intermediate grinding at the end of 50% of the total duration of heating, pelletization and hermetic sealing in copper tubes. Equilibrations were also carried out at 773 K with a total equilibration time of 960 h. Initially, these equilibrations were carried out in the vacuum sealed quartz tubes with samples contained in alumina crucibles. However, in most of the cases, the quartz tubes were severely attacked. Analysis of the deposits on the quartz tubes showed significant amounts of bismuth indicating the attack was due to Bi_2O_3 vapor. Since Cu_2O is thermodynamically less stable than Bi_2O_3 [ΔG° for the reaction: 6 Cu (s) + Bi_2O_3 (s) $\rightarrow$ 2 Bi (l) + 3 Cu_2O (s) is 24.6 kJ mol^{-1} at 773 K and 3.3 kJ mol^{-1} at 1023 K.], copper tubes were used to contain the samples taken in zirconia crucibles. The products obtained after equilibrations were analyzed by XRD. The compositions of the samples taken for equilibrations are shown in Fig. 2. The details of these experiments are given in Tables 4 and 5.

To confirm the phases that co-exist with liquid bismuth, samples were equilibrated with an excess of liquid bismuth also. Porous pellets of samples containing Bi metal powder as a constituent were prepared and were kept immersed in an excess of molten bismuth metal taken in alumina crucibles as described in section 3.2.3. Bismuth metal was taken as a constituent of the sample pellet to ensure good contact between the solid phases and the excess liquid metal in the crucible during equilibrations. These samples were prepared inside the argon atmosphere glove box. The samples were then taken outside the glove box, vacuum sealed in quartz ampoules and equilibrated. Since the pellets were immersed in excess liquid Bi, vaporization of Bi_2O_3 was minimum, and therefore they could be sealed in quartz ampoules. The initial overall compositions of the pellets are shown in Fig. 2. The composition and the initial phases present in the samples taken for equilibration at 1023 K are given in Table 4. The corresponding data on the samples equilibrated at 773 K are given in Table 5.

3.4. Oxygen potential measurements by emf method

With a view to study the temperature range of stability of $BiFeO_3$ and measure the Gibbs energy of formation of $BiFeO_3$ and $Bi_{25}FeO_{39}$, four emf cells using yttria stabilized zirconia solid electrolyte were constructed, and oxygen potentials were measured.

(-)W, Sample-1 |YSZ| (O_2, 1atm), Pt (+) (I)

(-)W, Sample-2 |YSZ| (O_2, 1atm), Pt (+) (II)

(-)W, Sample-3 |YSZ| (O_2, 1atm), Pt (+) (III)

(-)W, Sample-4 |YSZ| (O_2, 1atm), Pt (+) (IV)

For cell I, Bi, $Bi_2Fe_4O_9$ and $BiFeO_3$ (containing a small amount of $Bi_{25}FeO_{39}$) mixture was used as the sample electrode (sample 1), and for cell II, a mixture of Bi, $Bi_2Fe_4O_9$ and $Bi_{25}FeO_{39}$ was used as the sample electrode (sample 2). Two sample electrodes with

different compositions but falling within the section bound by Bi, $BiFeO_3$ and $Bi_{25}FeO_{39}$ were used for measurements with cell III and IV (samples 3 and 4). Emf values were measured in the temperature range of 773 to 1023 K. The details of the emf measurements are given in Table 6.

The details of the experimental assembly of the galvanic cell are discussed in Ref. [9]. One end closed yttria stabilized zirconia (YSZ) solid electrolyte tube having a flat bottom (13 mm OD, 9 mm ID and 300 mm long) supplied by M/s Nikkato Corporation, Japan was used. The reference electrode of the cell was prepared by applying platinum paste (M/s Eltecks Corporation, India) over the inner bottom surface of the electrolyte tube and heating it at 1373 K for 2 h in the air which resulted in a uniform and porous platinum film over the electrolyte surface. Pure oxygen gas was used as the reference. For sample electrodes, tungsten wire was used as an electrical lead. A sample electrode was prepared by mixing the starting materials in approximately equal volume ratios and by pelletizing it. The entire cell assembly was taken inside an argon atmosphere glove box. An appropriate quantity of Bi metal was melted in an alumina crucible, and the sample pellet was then forcibly dipped in liquid bismuth by placing the solid electrolyte tube over it in such a way that the lower end of the tungsten lead was dipped in liquid Bi. After slow cooling, the entire cell assembly was taken outside the glove box. During emf measurements, high purity argon and oxygen gases were passed through the sample and reference compartments, respectively. The cell assembly was placed in the constant temperature zone of a furnace. A 50 mm long, hollow cylindrical stainless steel block was also placed in the constant temperature zone of the furnace to further enhance the uniformity of the temperature in the zone. Using this arrangement the cell temperature could be controlled within ± 0.2 K using a PID temperature controller. The stainless steel block was grounded to avoid any ac pickup in the emf signal. The cell emf was measured using a high impedance electrometer (input impedance $>10^{14}\Omega$,

M/s Keithley, U.S.A, Model-6514) and the temperature was measured using a multimeter (M/s Agilent Technologies, Malaysia, Model- 34970A Data acquisition/switch unit). Data were recorded using a computer interface. Attainment of equilibrium was tested by shorting the two electrical leads and testing for the restoration of the pre-test emf. The readings were recorded when the cell emf was stable within ± 0.05 mV for at least 6 h. The thermo emf due to dissimilar electrical leads viz., platinum and tungsten were measured separately by forming a junction between the two electrical leads followed by the measurement of the thermo emf between them as a function of temperature. Using this data, the measured cell EMF was corrected to derive the actual EMF.

Before and after completion of the emf measurements (which involved multiple heating and cooling cycles), the sample electrodes were analyzed by XRD.

4. Results and discussion

4.1. Characterization of the ternary compounds

The XRD patterns of $Bi_2Fe_4O_9$ prepared by solid-state reaction method and co-precipitation route and $Bi_{25}FeO_{39}$ prepared by solid-state reaction method matched exactly with the patterns reported in JCPDS files 74-1098 and 46-0416, respectively [33]. Phase pure sample of $BiFeO_3$ could not be prepared by both the methods. XRD pattern of $BiFeO_3$ sample showed the presence of a small amount of $Bi_{25}FeO_{39}$ also. Except for the peaks of $Bi_{25}FeO_{39}$, all other peaks in the XRD pattern obtained for the $BiFeO_3$ sample matched with the pattern, 77-4078 reported in JCPDS file. The XRD patterns of the compounds prepared by the solid-state reaction of oxides are compared with their PCPDF patterns in Fig. 3. SEM/EDS analysis of $Bi_{25}FeO_{39}$ and $Bi_2Fe_4O_9$ showed uniform phase distribution with no impurity phases, and the composition was found to be homogeneous with 5% uncertainty.

The analysis results of ICP-AES showed that the total metallic impurities are less than 2 ppm and Bi to Fe ratios in $Bi_{25}FeO_{39}$ and $Bi_2Fe_4O_9$ were 25.0 ± 1.4 and 0.50 ± 0.03.

4.2. Experiments to determine the temperature range of stability of $BiFeO_3$

4.2.1. TG/DTA and DSC experiments with $BiFeO_3$

The thermogram obtained by TG/DTA of $BiFeO_3$ from 298 to 973 K did not show any weight change as well as any thermal event both on heating and cooling. XRD pattern of $BiFeO_3$ after the TG/DTA experiment also did not show any change from its XRD pattern taken prior to the experiment. The thermogram from DSC experiment in the temperature range of 298 to 823 K also gave the same results. This could mean either $BiFeO_3$ is thermodynamically stable in the temperature range of study or the kinetics of its decomposition is too slow that it did not decompose within the short dwell time of the sample during TG/DTA and DSC experiments at high temperatures.

4.2.2. Equilibration of $BiFeO_3$ in the vacuum and air at different temperatures

As described in section 3.2.2, nine samples of $BiFeO_3$ were simultaneously equilibrated for prolonged periods in a temperature gradient furnace in the vacuum to determine its temperature range of stability. Similar equilibrations were carried out in the air also. The results obtained are given in Tables 1 and 2. As mentioned in section 4.1, phase pure $BiFeO_3$ could not be prepared and it always contained a small amount of $Bi_{25}FeO_{39}$. XRD patterns obtained after equilibrating the samples in the vacuum and air are shown in Figs. 4 and 5, respectively. The pattern of the samples equilibrated at temperatures below 763 K in the vacuum (samples 1 to 3 in Table 1) was identical to that of the starting material, i.e., a mixture of $BiFeO_3$ (major phase) and $Bi_{25}FeO_{39}$ (minor phase). A similar feature is observed for samples equilibrated in the air at 757 K and below (samples 10 to 13 in Table 2). In the case of the sample which was equilibrated in the vacuum at 763 K, the intensity of

XRD lines of $Bi_{25}FeO_{39}$ increased along with those of $Bi_2Fe_4O_9$. Simultaneously, a reduction in the intensity of the lines corresponding to $BiFeO_3$ was also observed. This shows the decomposition of $BiFeO_3$ to the neighboring compounds, namely $Bi_{25}FeO_{39}$ and Bi_2FeO_9. But this decomposition was not complete even after 480 h. A similar feature is observed in the sample equilibrated in the air at 807 K. In the case of the samples equilibrated at 805 and 871 K in the vacuum, and 853 K in the air, $BiFeO_3$ had decomposed completely to $Bi_{25}FeO_{39}$ and Bi_2FeO_9. In the case of sample equilibrated at 943 K in the vacuum and at 941 K in the air, the presence of a small amount of $BiFeO_3$ could be identified although major phases are $Bi_{25}FeO_{39}$ and $Bi_2Fe_4O_9$. In the case of samples equilibrated at higher temperatures, $BiFeO_3$ was the major phase although small quantities of the other two phases could be identified. These results indicate that the kinetics of decomposition of $BiFeO_3$ is very sluggish and it appears as a metastable compound at low temperatures. It appears as a thermodynamically stable phase only at temperatures around 940 K. These results are in agreement with those reported by Maurya et al. [30] and Egorysheva et al. [31]. In their work, the authors observed the formation of $BiFeO_3$ at temperatures between 873 and 973 K. Although $BiFeO_3$ could be prepared as a metastable phase by heating the hydroxides at 773 K for shorter periods (section 3.1), it is found to decompose, although not to completion, on prolonged heating at 763 K (section 3.2.2) [Table 2 shows reactions between Bi_2O_3 and Fe_2O_3 only]. This could presumably because of the small Gibbs energy change for the decomposition reaction given below and its slow kinetics resulting in metastability of $BiFeO_3$ at low temperatures:

$$49\ BiFeO_3 \rightarrow 12\ Bi_2Fe_4O_9 + Bi_{25}FeO_{39}$$

The sluggish kinetics of decomposition of $BiFeO_3$ as well as its formation from the decomposition products have been exemplified by the results of the emf measurements also

(discussed in section 4.4). Further experiments are required to determine the exact temperature above which $BiFeO_3$ becomes a thermodynamically stable phase.

4.2.3. Equilibration of samples containing $BiFeO_3$ with liquid Bi

XRD patterns obtained after equilibrating mixtures of Bi, $Bi_2Fe_4O_9$ and $BiFeO_3$ in liquid Bi at 873 and 1023 K for 480 h are shown in Fig. 6, and the results are summarized in Table 3. At 873 K, the intensity of the lines corresponding to $BiFeO_3$ had drastically reduced, and the intensities of the lines of $Bi_2Fe_4O_9$ and $Bi_{25}FeO_{39}$ had increased. At 1023 K, the intensity of the lines of $Bi_{25}FeO_{39}$ had decreased, and those of $BiFeO_3$ had increased. This is in agreement with the observations made during equilibrations of $BiFeO_3$ in the air and vacuum described in section 4.2.2.

XRD patterns obtained after equilibrating mixtures of Bi, $BiFeO_3$ and $Bi_{25}FeO_{39}$ in liquid Bi at 873 and 1023 K are shown in Fig. 7 and the results are given in Table 3. At 1023 K, $BiFeO_3$ had not decomposed, but at 873 K, it decomposed almost completely and the other two phases, i.e., $Bi_2Fe_4O_9$ and $Bi_{25}FeO_{39}$ had formed. This is again in agreement with the results of long term equilibration of $BiFeO_3$ in the air and vacuum described in the earlier section. These results also confirm that $BiFeO_3$ is metastable at low temperatures and would become stable only at high temperatures.

4.3 Additional phase equilibration studies

Results of long term equilibrations of samples with compositions falling in the section bound by Bi, $Bi_2Fe_4O_9$ and Bi_2O_3 at 1023 K are given in Table 4. XRD analysis of samples 1 and 2 after equilibration showed the presence of a major amount of Bi, $Bi_2Fe_4O_9$ and $BiFeO_3$ and a small amount of $Bi_{25}FeO_{39}$. It is to be pointed out that the experiments to prepare $BiFeO_3$ (described in section 4.1), always yielded a small amount of $Bi_{25}FeO_{39}$ also.

XRD analysis of samples 3 and 4, after equilibration showed the presence of Bi, $BiFeO_3$ and $Bi_{25}FeO_{39}$, indicating the coexistence of these phases at 1023 K. Phases present in samples 5 to 7, after their equilibration, confirmed the presence of Bi-$Bi_{25}FeO_{39}$-Bi_2O_3 phase field at 1023 K. From these results, the phase fields identified in the region bound by Bi, $Bi_2Fe_4O_9$ and Bi_2O_3 at 1023 K are: 1) Bi-$BiFeO_3$-$Bi_{25}FeO_{39}$ and 2) Bi-$Bi_{25}FeO_{39}$-Bi_2O_3. According to the long term equilibrations of $BiFeO_3$ discussed above, $BiFeO_3$ is stable at 1023 K. Present experiments have also established the thermodynamic stability of $BiFeO_3$ at this temperature. However, the existence of Bi-$Bi_2Fe_4O_9$-$BiFeO_3$ phase field was not evident in any of the equilibration studies at 1023 K, but its existence can be deduced since (i) the existence of Bi-$Bi_2Fe_4O_9$-Fe_2O_3 and Bi-$BiFeO_3$-$Bi_{25}FeO_{39}$ phase fields have been confirmed by the long term equilibrations and (ii) the coexistence of $Bi_2Fe_4O_9$ and $BiFeO_3$, and $BiFeO_3$ and $Bi_{25}FeO_{39}$ has been established by long term equilibration of different molar ratios of Bi_2O_3 and Fe_2O_3 in the air in the authors' previous work (discussed in section 4.2 of Ref. [9]).

Results of equilibrations at 773 K are summarized in Table 5, and they need to be considered in light of long term equilibrations of $BiFeO_3$ discussed above. Equilibrations at 773 K also showed the same results as in the case of equilibrations at 1023 K. Samples, 8 and 9 (in Table 5) whose compositions were in the region bound by Bi, $Bi_2Fe_4O_9$ and $BiFeO_3$, gave a mixture of Bi, $Bi_2Fe_4O_9$, $BiFeO_3$ and a small amount of $Bi_{25}FeO_{39}$. Sample 10, whose composition was in the region bound by Bi, $BiFeO_3$ and $Bi_{25}FeO_{39}$, after equilibration, gave a mixture of Bi, $BiFeO_3$ and $Bi_{25}FeO_{39}$, indicating the coexistence of these phases at 773 K. Samples 11 and 12, confirmed the presence of the phase field: Bi-$Bi_{25}FeO_{39}$-Bi_2O_3 at 773 K. From these results, the presence of the following phase fields was identified at 773 K: (a) Bi-$BiFeO_3$-$Bi_{25}FeO_{39}$ and (b) Bi-$Bi_{25}FeO_{39}$-Bi_2O_3. Since $BiFeO_3$ is metastable at 773 K, the phase which will be coexisting with Bi and $Bi_2Fe_4O_9$ will be

$Bi_{25}FeO_{39}$, but none of the equilibrations proved the existence of Bi-$Bi_2Fe_4O_9$-$Bi_{25}FeO_{39}$ phase field at 773 K. However, the existence of Bi-$Bi_2Fe_4O_9$-Fe_2O_3 and Bi-$Bi_{25}FeO_{39}$-Bi_2O_3 phase fields had been established by the long term equilibration studies. Further, the equilibration of different molar ratios of Bi_2O_3 and Fe_2O_3 in the air (discussed in section 4.2 of ref. 9) indicated that no other ternary compounds with their composition falling in between $Bi_2Fe_4O_9$ and $Bi_{25}FeO_{39}$ are present at 773 K. All these observations lead to the confirmation of the existence of Bi-$Bi_2Fe_4O_9$-$Bi_{25}FeO_{39}$ phase field at 773 K.

Based on all the above results, the ternary phase diagram of Bi-Fe-O system at 773 and 1023 K have been constructed and are shown in Figs. 8 and 9. The results of the experiments showed that on increasing the oxygen content of bismuth metal in equilibrium with iron metal, iron oxides would first appear as the coexisting phases. With further increase in oxygen content in bismuth, $Bi_2Fe_4O_9$ would appear as the coexisting phase.

4.4. Emf measurements

To determine the temperature above which $BiFeO_3$ appear as a thermodynamically stable phase in liquid Bi and also to determine the Gibbs energy of formation of $BiFeO_3$ and $Bi_{25}FeO_{39}$, oxygen potentials in liquid Bi in equilibrium with different phases were measured. The details of the emf measurements are given in Table 6 and the output of the emf cells, namely I, II, III, and IV in the chronological order of measurements along with the dwell time at each temperature are given in Tables 7 to 10. The variation of emf output of these cells with temperature is shown in Fig. 10. As seen in Tables 7 to 10, all the cells were first operated at temperatures above 1000 K where $BiFeO_3$ would be thermodynamically stable. The values of emf and its temperature dependence in all the cells were nearly the same, as seen from Fig. 10. As seen from Table 6, overall compositions of the samples for

the cells were chosen such that in cell - I and II, they would lie in the region bound by Bi, $Bi_2Fe_4O_9$ and $BiFeO_3$. In cells III and IV, the overall compositions would lie in the region bound by Bi, $BiFeO_3$ and $Bi_{25}FeO_{39}$.

From the results of the experiments discussed in the earlier section, it is known that $BiFeO_3$ would appear as the stable phase at a temperature around 940 K. Hence, when equilibrium is established at temperatures below about 940 K, samples in all the four cells are expected to belong to Bi-$Bi_2Fe_4O_9$-$Bi_{25}FeO_{39}$ phase field. At temperatures above about 940 K, the cell I and II are expected to belong to Bi-$Bi_2Fe_4O_9$-$BiFeO_3$ phase field, while the samples of cells III and IV are expected to belong to the Bi-$BiFeO_3$-$Bi_{25}FeO_{39}$ phase field. Since the temperature dependence of oxygen potentials in all the three phase fields are expected to be different, a slope change at the temperature of appearance of $BiFeO_3$ as the stable phase is expected. However, as seen from Fig. 10, no significant change in slope has been observed.

It is seen from Table 7 and 8, the final temperatures of operation of the cell I and II were 985.5 and 1024.6 K, respectively. At these temperatures, $BiFeO_3$ is expected to be present as a stable phase. When the cells III and IV were cooled to room temperature from 801.4 and 859.6 K, respectively, $BiFeO_3$ is not expected to be present. However, XRD patterns of the samples retrieved from all the four cells showed the presence of Bi, $BiFeO_3$ and $Bi_{25}FeO_{39}$ in them. Cells I and II contained additionally $Bi_2Fe_4O_9$ as seen from Table 6. It is seen that metastable phases were present in the samples. This could be due to insufficient dwell time at low operating temperatures of the cell for the metastable phases to decompose completely, although emf values were stable due to the ‘equilibrium’ established

with these phases. Due to the identical 'equilibrium' conditions in all the four cells, emf values and their temperature dependence were the same. Obviously, these data could not be used to deduce the Gibbs energy of formation of $BiFeO_3$ and $Bi_{25}FeO_{39}$.

5. Conclusions

The thermal stability of $BiFeO_3$ has been examined by different experimental techniques and found that it is metastable at low temperatures and become stable only around 940 K. The isothermal sections of the ternary phase diagram of Bi-Fe-O system at 773 and 1023 K have been constructed based on long term equilibration studies.

Acknowledgments

The authors are thankful to Mr. Khaja Mohideen, Mr. N. Eswaran, and Mr. K. Haridas, for their help in constructing the emf cell. The authors sincerely acknowledge Mr. Henson Raj for his help in helium leak testing of the emf cell assembly. One of the authors (AVM) acknowledges the Department of Atomic Energy, India, for providing financial support.

References

1. B.F. Gromov (Ed), Heavy Liquid Metal Coolants in Nuclear Technology (HLMC 98), vols.1&2, SSC RF-IPPE, Obninsk,1999.
2. N. Li, Active control of oxygen in molten lead–bismuth eutectic systems to prevent steel corrosion and coolant contamination, J. Nucl. Mater. 300 (2002) 73-81.
3. S.K. Sahu, R. Ganesan, T. Gnanasekaran, Studies on phase diagram of Pb–Cr–O system, J. Nucl. Mater. 376 (2008) 366-370.

4. S.K. Sahu, R. Ganesan, T. Gnanasekaran, Standard molar Gibbs free energy of formation of Pb_5CrO_8 (s), Pb_2CrO_5 (s), and $PbCrO_4$ (s), J. Chem. Thermodyn. 42 (2010) 1-7.

5. S.K. Sahu, R. Ganesan, T.G. Srinivasan, T. Gnanasekaran, The standard molar enthalpies of formation of Pb_2CrO_5 (s) and Pb_5CrO_8 (s) by acid solution calorimetry, J. Chem. Thermodyn. 43 (2011) 750-753.

6. S.K. Sahu, R. Ganesan, T. Gnanasekaran, Studies on the phase diagram of Pb–Fe–O system and standard molar Gibbs energy of formation of '$PbFe_5O_{8.5}$' and $Pb_2Fe_2O_5$, J. Nucl. Mater. 426 (2012) 214-222.

7. S.K. Sahu, M. Sahu, R.S. Srinivasa, T. Gnanasekaran, Determination of heat capacities of $PbCrO_4$ (s), Pb_2CrO_5 (s), and Pb_5CrO_8 (s), Monatsh. Chem. 143 (2012) 1207-1214.

8. S.K. Sahu, R. Ganesan, T. Gnanasekaran, The standard molar enthalpies of formation of $Pb_2Fe_2O_5$ (s) and $PbFe_5O_{8.5}$ (s) by acid solution calorimetry, J. Chem. Thermodyn. 56 (2013) 57-59.

9. A.V. Meera, R. Ganesan, T. Gnanasekaran, Partial phase diagram of Bi-Fe-O system and the standard molar Gibbs energy of formation of $Bi_2Fe_4O_9$, J. Alloys Compd. 692 (2017) 841-847.

10. E.M. Levin, R.S. Roth, Polymorphism of bismuth sesquioxide. II. Effect of Oxide additions on the polymorphism of Bi_2O_3, J. Res. Nat. Bur. Std. US 68A (1964) 197-206.

11. H. Koizumi, N. Niizeki, T. Ikeda, X-ray study on Bi_2O_3-Fe_2O_3 system, Jpn. J. Appl. Phys. 3 (1964) 495-496.

12. E.I. Speranskaya, V.M. Skorikov, E.Y. Rode, V.A. Terekhova, The phase diagram of the system bismuth oxide-ferric oxide, Bull. Acad. Sci. USSR, Div. Chem. Sci. (Engl. Transl.) 5 (1965) 905-906.

13. T.M. Bruton, J.C. Brice, O.F. Hill, P.A.C. Whiffin, Flux growth of some γ-Bi_2O_3 crystals by the top seeded technique, J. Cryst. Growth 23 (1974) 21-24.

14. D.C. Craig, N.C. Stephenson, Structural studies of some body-centered cubic phases of mixed oxides involving Bi_2O_3: The structures of $Bi_{25}FeO_{40}$ and $Bi_{38}ZnO_{60}$, J. Solid State Chem. 15 (1975) 1-8.

15. A. Ramanan, J. Gopalakrishnan, Low-temperature preparation of sillenite phases in Bi-M-O (M = Mn, Fe, Co) systems, Ind. J. Chem. 24A (1985) 594-596.

16. S.F. Radaev, L.A. Muradyan, V.I. Simonov, Atomic structure and crystal chemistry of sillenites: $Bi_{12}\left(Bi^{3+}_{0.50}Fe^{3+}_{0.50}\right)O_{19.50}$ and $Bi_{12}\left(Bi^{3+}_{0.67}Zn^{2+}_{0.33}\right)O_{19.33}$, Acta Cryst. B47 (1991) 1-6.

17. A. Maitre, M. Francois, J.C. Gachon, Experimental study of the Bi_2O_3-Fe_2O_3 pseudo-binary system, J. Phase Equilib. Diff. 25 (2004) 59-67.

18. R. Palai, R.S. Katiyar, H. Schmid, P. Tissot, S.J. Clark, J. Robertson, S.A.T. Redfern, G. Catalan, J.F. Scott, β phase and γ-β metal–insulator transition in multiferroic $BiFeO_3$, Phys. Rev. B 77 (2008) 014110 1-11.

19. J. Lu, L.J. Qiao, P.Z. Fu, Y.C. Wu, Phase equilibrium of Bi_2O_3–Fe_2O_3 pseudo-binary system and growth of $BiFeO_3$ single crystal, J. Cryst. Growth 318 (2011) 936-941.

20. S. Phapale, R. Mishra, D. Das, Standard enthalpy of formation and heat capacity of compounds in the pseudo-binary Bi_2O_3–Fe_2O_3 system, J. Nucl. Mater. 373 (2008) 137-141.

21. Q. Zhang, D. Sando, V. Nagarajan, Chemical route derived bismuth ferrite thin films and nanomaterials, J. Mater. Chem. C: Mater. Opt. Electron. Devices 4 (2016) 4092-4124.

22. J. Wu, Z. Fan, D. Xiao, J. Zhu, J. Wang, Multiferroic bismuth ferrite-based materials for multifunctional applications: Ceramic bulks, thin films and nanostructures, Prog. Mater. Sci. 84 (2016) 335-402.

23. A. Molak, D. K. Mahato, A.Z. Szeremeta, Synthesis and characterization of electrical features of bismuth manganite and bismuth ferrite: effects of doping in cationic and anionic sublattice: Materials for applications, Prog. Cryst. Growth Char. Mater. 64 (2018) 1-22.

24. G.D. Achenbach, W.J. James, R. Gerson, Preparation of single-phase polycrystalline $BiFeO_3$, J. Am. Ceram. Soc. 50 (1967) 437.

25. J. De Sitter, C. Dauwe, E. De Grave, A. Govaert, G. Robbrecht, On the magnetic properties of the basic compounds in the Fe_2O_3-Bi_2O_3 system, Physica 86-88 B (1977) 919-920.

26. M.I. Morozov, N.A. Lomanova, V.V. Gusarov, Specific features of $BiFeO_3$ formation in a mixture of bismuth (III) and iron (III) oxides, Russ. J. Gen. Chem. 73 (2003) 1676-1680.

27. M. Valant, A.K. Axelsson, N. Alford, Peculiarities of a solid state synthesis of multiferroic polycrystalline $BiFeO_3$, Chem. Mater. 19 (2007) 5431-5436.

28. T.T. Carvalho, P.B. Tavares, Synthesis and thermodynamic stability of multiferroic $BiFeO_3$, Mater. Lett. 62 (2008) 3984-3986.

29. S.M. Selbach, M. Einarsrud, T. Grande, On the thermodynamic stability of $BiFeO_3$, Chem. Mater. 21 (2009) 169-173.

30. D. Maurya, H. Thota, K.S. Nalwa, A. Garg, $BiFeO_3$ ceramics synthesized by mechanical activation assisted versus conventional solid state reaction process: A comparative study, J. Alloy. Comp. 477 (2009) 780-784.

31. A.V. Egorysheva, V.D. Volodin, O.G. Ellert, N.N. Efimov, V.M. Skorikov, A.E. Baranchikov, V.M. Novotortsev, Mechanochemical activation of starting oxide mixtures for solid - state synthesis of $BiFeO_3$, Inorg. Mater. 49 (2013) 303-309.

32. N.A. Lemonova, V.V. Gusarov, Influence of synthesis temperature on $BiFeO_3$ nanoparticles formation, Nanosystems: Phys. Chem. Math. 4 (2013) 696-705.

33. PDF-4+ database, International Centre for Diffraction Data, 2015.

ACCEPTED MANUSCRIPT

Table 1 Phases formed after equilibration of $BiFeO_3$ (containing small amount of $Bi_{25}FeO_{39}$) in vacuum for 480 h

Sample no.	Temperature (K)	Phases identified after equilibration
1	716	$BiFeO_3$ (major phase), $Bi_{25}FeO_{39}$ (minor phase)
2	722	$BiFeO_3$ (major phase), $Bi_{25}FeO_{39}$ (minor phase)
3	726	$BiFeO_3$ (major phase), $Bi_{25}FeO_{39}$ (minor phase)
4	763	$BiFeO_3$, $Bi_{25}FeO_{39}$, $Bi_2Fe_4O_9$
5	805	$Bi_{25}FeO_{39}$, $Bi_2Fe_4O_9$
6	871	$Bi_{25}FeO_{39}$, $Bi_2Fe_4O_9$
7	943	$BiFeO_3$ (minor phase), $Bi_{25}FeO_{39}$ (major phase), $Bi_2Fe_4O_9$ (major phase)
8	1034	$BiFeO_3$ (major phase), $Bi_{25}FeO_{39}$ (minor phase), $Bi_2Fe_4O_9$ (minor phase)
9	1089	$BiFeO_3$ (major phase), $Bi_{25}FeO_{39}$ (minor phase), $Bi_2Fe_4O_9$ (minor phase)

ACCEPTED MANUSCRIPT

Table 2 Phases formed after equilibration of $BiFeO_3$ (containing small amount of $Bi_{25}FeO_{39}$) in air for 480 h

Sample no.	Temperature (K)	Phases identified after equilibration
10	716	$BiFeO_3$ (major phase), $Bi_{25}FeO_{39}$ (minor phase)
11	722	$BiFeO_3$ (major phase), $Bi_{25}FeO_{39}$ (minor phase)
12	725	$BiFeO_3$ (major phase), $Bi_{25}FeO_{39}$ (minor phase)
13	757	$BiFeO_3$ (major phase), $Bi_{25}FeO_{39}$ (minor phase)
14	807	$BiFeO_3$, $Bi_{25}FeO_{39}$, $Bi_2Fe_4O_9$
15	853	$Bi_{25}FeO_{39}$, $Bi_2Fe_4O_9$
16	941	$BiFeO_3$ (minor phase), $Bi_{25}FeO_{39}$ (major phase), $Bi_2Fe_4O_9$ (major phase)
17	1028	$BiFeO_3$ (major phase), $Bi_{25}FeO_{39}$ (minor phase), $Bi_2Fe_4O_9$ (minor phase)
18	1085	$BiFeO_3$ (major phase), $Bi_{25}FeO_{39}$ (minor phase), $Bi_2Fe_4O_9$ (minor phase)

Table 3 Results of equilibration of Bi, $Bi_2Fe_4O_9$, $BiFeO_3$ and Bi, $BiFeO_3$, $Bi_{25}FeO_{39}$ mixtures in liquid Bi

Starting materials and their mole ratio	Temperature (K)	Phases identified after equilibrating in liq. Bi for 480 h
Bi, $Bi_2Fe_4O_9$, $BiFeO_3$ (1 : 0.6 : 2) (Overall composition within the area bound by Bi, $Bi_2Fe_4O_9$ and $BiFeO_3$)	873	Bi, $Bi_2Fe_4O_9$, $BiFeO_3$ (minor phase), $Bi_{25}FeO_{39}$
	1023	Bi, $Bi_2Fe_4O_9$, $BiFeO_3$, $Bi_{25}FeO_{39}$ (minor phase)
Bi, $BiFeO_3$, $Bi_{25}FeO_{39}$ (1 : 1.56 : 0.1) (Overall composition within the area bound by Bi, $BiFeO_3$ and $Bi_{25}FeO_{39}$)	873	Bi, $BiFeO_3$ (minor phase), $Bi_{25}FeO_{39}$, $Bi_2Fe_4O_9$ (minor phase)
	1023	Bi, $BiFeO_3$, $Bi_{25}FeO_{39}$

ACCEPTED MANUSCRIPT

ACCEPTED MANUSCRIPT

Table 4 Details of equilibration of samples with compositions in the section bound by Bi, $Bi_2Fe_4O_9$ and Bi_2O_3 at 1023 K

Sample no.	Composition	Phases taken before equilibration	Duration of equilibration (h)	Phases identified after equilibration
1	$Bi_{0.280}Fe_{0.200}O_{0.520}$	Bi_2O_3, Fe, Fe_2O_3	480	Bi, $Bi_2Fe_4O_9$, $BiFeO_3$, $Bi_{25}FeO_{39}$ (minor)
2	$Bi_{0.213}Fe_{0.222}O_{0.565}$*	Bi, Fe_2O_3, Bi_2O_3 in liq. Bi	480	Bi, $Bi_2Fe_4O_9$, $BiFeO_3$, $Bi_{25}FeO_{39}$ (minor)
3	$Bi_{0.335}Fe_{0.095}O_{0.570}$	Bi_2O_3, Fe, Fe_2O_3	480	Bi,$BiFeO_3$, $Bi_{25}FeO_{39}$
4	$Bi_{0.470}Fe_{0.090}O_{0.440}$*	Bi, Fe, Bi_2O_3 in liq. Bi	480	Bi,$BiFeO_3$, $Bi_{25}FeO_{39}$
5	$Bi_{0.550}Fe_{0.005}O_{0.445}$	Bi, $Bi_2Fe_4O_9$, Bi_2O_3	480	Bi, $Bi_{25}FeO_{39}$, Bi_2O_3
6	$Bi_{0.550}Fe_{0.005}O_{0.445}$*	Bi, Fe_2O_3, $BiFeO_3$ in liq. Bi	480	Bi, $Bi_{25}FeO_{39}$, Bi_2O_3
7	$Bi_{0.550}Fe_{0.005}O_{0.445}$*	Bi, Fe, Bi_2O_3 in liq. Bi	480	Bi, $Bi_{25}FeO_{39}$, Bi_2O_3

* Overall composition of the phase mixture taken in the form of pellet which was equilibrated with excess of liquid Bi. Samples sealed in quartz ampoules.

ACCEPTED MANUSCRIPT

Table 5 Details of equilibration of samples with compositions in the section bound by Bi, $Bi_2Fe_4O_9$ and Bi_2O_3 at 773 K

Sample no.	Composition	Phases taken before equilibration	Duration of equilibration (h)	Phases identified after equilibration
8	$Bi_{0.280}Fe_{0.200}O_{0.520}$*	Bi_2O_3, Fe, Fe_2O_3 in liq. Bi	480	Bi,$Bi_2Fe_4O_9$, $BiFeO_3$, $Bi_{25}FeO_{39}$ (minor)
9	$Bi_{0.394}Fe_{0.174}O_{0.432}$*	Bi, Fe, Bi_2O_3 in liq. Bi	480	Bi,$Bi_2Fe_4O_9$, $BiFeO_3$, $Bi_{25}FeO_{39}$ (minor)
10	$Bi_{0.470}Fe_{0.090}O_{0.440}$*	Bi, Fe, Bi_2O_3 in liq. Bi	480	Bi, $BiFeO_3$, $Bi_{25}FeO_{39}$
11	$Bi_{0.550}Fe_{0.005}O_{0.445}$	Bi, $Bi_2Fe_4O_9$, Bi_2O_3	960	Bi, $Bi_{25}FeO_{39}$, Bi_2O_3
12	$Bi_{0.550}Fe_{0.005}O_{0.445}$*	Bi, Fe_2O_3, $BiFeO_3$ in liq. Bi	480	Bi, $Bi_{25}FeO_{39}$, Bi_2O_3

* Overall composition of the phase mixture taken in the form of pellet which was equilibrated with excess of liquid Bi. Samples sealed in quartz ampoules.

ACCEPTED MANUSCRIPT

ACCEPTED MANUSCRIPT

Table 6 Details of emf measurements

No	Starting materials	Region in which overall composition would lie	Total duration of measurement	Phases identified after emf measurement
Cell I	Bi, $Bi_2Fe_4O_9$, $BiFeO_3$ (containing small amount of $Bi_{25}FeO_{39}$)	Bi-$Bi_2Fe_4O_9$-$BiFeO_3$	22 days (17 data points)	Bi, $Bi_2Fe_4O_9$, $BiFeO_3$, $Bi_{25}FeO_{39}$ (minor phase)
Cell II	Bi, $Bi_2Fe_4O_9$, $Bi_{25}FeO_{39}$	Bi-$Bi_2Fe_4O_9$-$BiFeO_3$	3 months (33 data points)	Bi, $Bi_2Fe_4O_9$ (major phase), $BiFeO_3$ (minor phase) $Bi_{25}FeO_{39}$ (minor phase)
Cell III	Bi, $BiFeO_3$ (containing small amount of $Bi_{25}FeO_{39}$), $Bi_{25}FeO_{39}$	Bi-$BiFeO_3$–$Bi_{25}FeO_{39}$	2 months (20 data points)	Bi, $BiFeO_3$, $Bi_{25}FeO_{39}$
Cell IV	Bi, $BiFeO_3$ (containing small amount of $Bi_{25}FeO_{39}$), $Bi_{25}FeO_{39}$	Bi-$BiFeO_3$–$Bi_{25}FeO_{39}$	17 days (12 data points)	Bi, $BiFeO_3$, $Bi_{25}FeO_{39}$

ACCEPTED MANUSCRIPT

ACCEPTED MANUSCRIPT

Table 7 Output of cell I as a function of temperature

No.	Temperature (K)	Dwell time (h)	Emf (mV)
1	1013.3	37	504.5
2	930.0	23	541.2
3	822.3	40	594.4
4	780.0	25	615.0
5	868.0	24	572.0
6	969.5	18	522.0
7	998.8	46	510.8
8	955.7	25	529.3
9	897.8	63	557.4
10	852.4	27	579.9
11	803.5	27	603.4
12	777.9	21	615.5
13	837.4	22	586.7
14	882.3	39	564.8
15	913.6	22	549.6
16	943.4	12	535.0
17	985.5	14	515.2

ACCEPTED MANUSCRIPT

ACCEPTED MANUSCRIPT

Table 8 Output of cell II as a function of temperature

No.	Temperature (K)	Dwell time (h)	Emf (mV)	No.	Temperature (K)	Dwell time (h)	Emf (mV)
1	1023.7	179	501.8	18	773.1	28	616.7
2	1000.0	84	511.4	19	798.2	33	604.4
3	981.9	26	517.4	20	810.2	29	598.4
4	956.5	26	528.3	21	836.2	18	587.1
5	930.9	60	540.8	22	861.2	20	577.0
6	903.6	46	554.5	23	888.2	64	562.5
7	923.2	28.5	545.1	24	785.1	22	606.2
8	965.6	24	524.3	25	1018.1	48	500.2
9	939.8	48	536.0	26	998.1	49	508.6
10	1012.5	117	506.1	27	781.7	64	610.4
11	992.2	141	515.1	28	924.3	26	544.0
12	955.5	28	528.6	29	826.3	15	589.8
13	948.7	22	532.0	30	876.6	23	568.4
14	918.0	26	547.2	31	797.1	20	602.9
15	873.5	28	567.4	32	973.4	50	520.0
16	848.2	20	577.5	33	1024.6	26	498.7
17	823.2	164	589.1				

ACCEPTED MANUSCRIPT

ACCEPTED MANUSCRIPT

Table 9 Output of cell III as a function of temperature

No.	Temperature (K)	Dwell time (h)	Emf (mV)	No.	Temperature (K)	Dwell time (h)	Emf (mV)
1	1014.3	14	498.8	11	790.5	46	611.2
2	915.4	54	547.7	12	778.8	73	617.7
3	818.4	46	597.1	13	952.9	26	529.7
4	766.0	120	623.5	14	927.8	22	542.3
5	865.5	7	573.0	15	996.0	40	509.0
6	965.3	20	523.4	16	902.6	71	555.1
7	806.8	42	602.4	17	877.8	20	567.2
8	980.5	20	516.4	18	852.0	67	580.7
9	939.9	93	536.4	19	829.4	50	592.6
10	889.6	39	561.0	20	801.4	42	606.2

Table 10 Output of cell IV as a function of temperature

No.	Temperature (K)	Dwell time (h)	Emf (mV)
1	1020.6	17	497.0
2	921.5	22	545.5
3	828.1	19	590.0
4	783.8	47	611.5
5	874.6	55	568.5
6	969.1	18	522.0
7	998.4	42	507.3
8	950.8	6	530.9
9	945.4	12	533.8
10	804.2	24	601.4
11	896.0	21	557.9
12	859.6	24	576.2

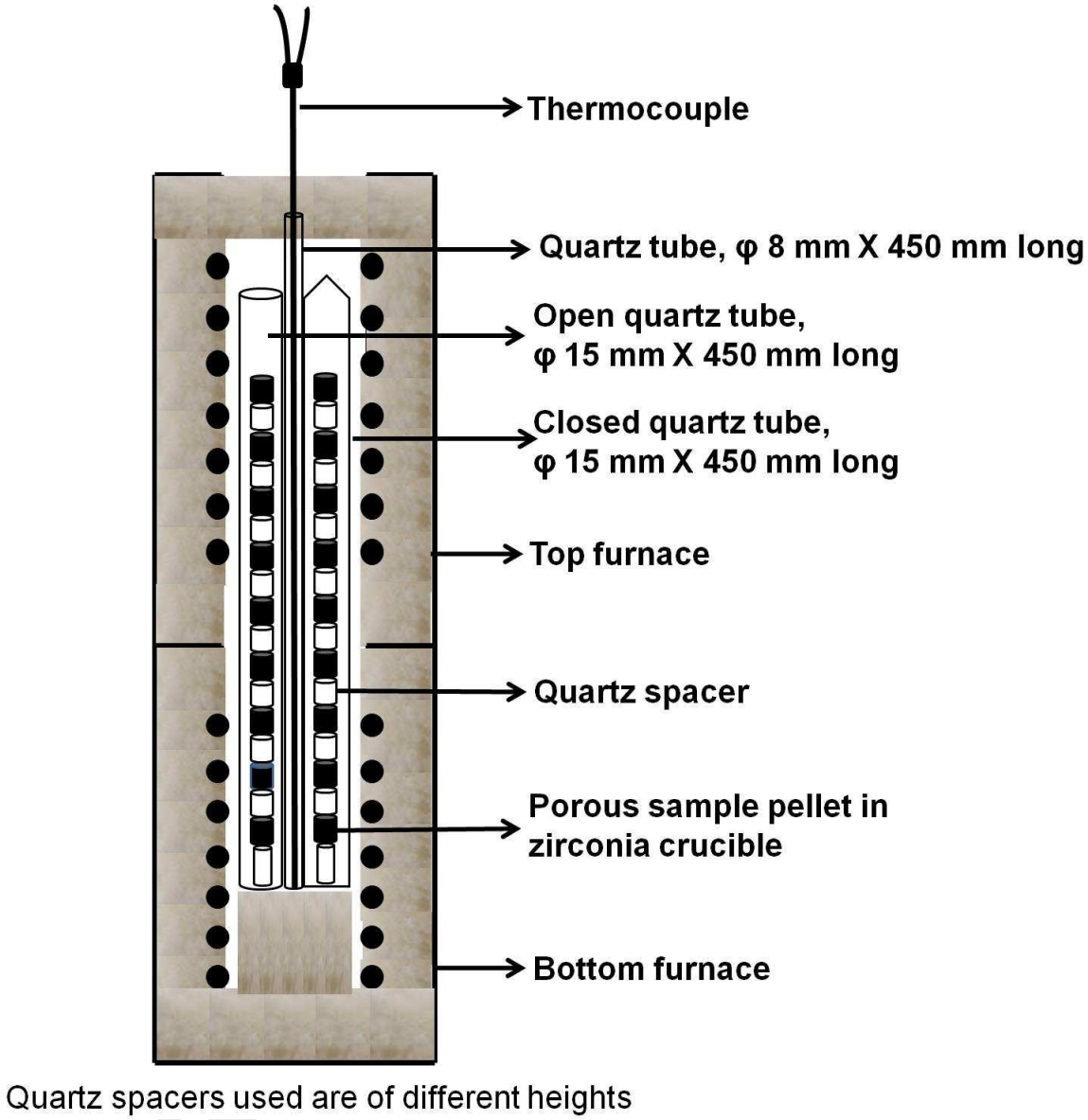

Fig. 1 Schematic of the experimental setup used for equilibrating $BiFeO_3$ at different temperatures

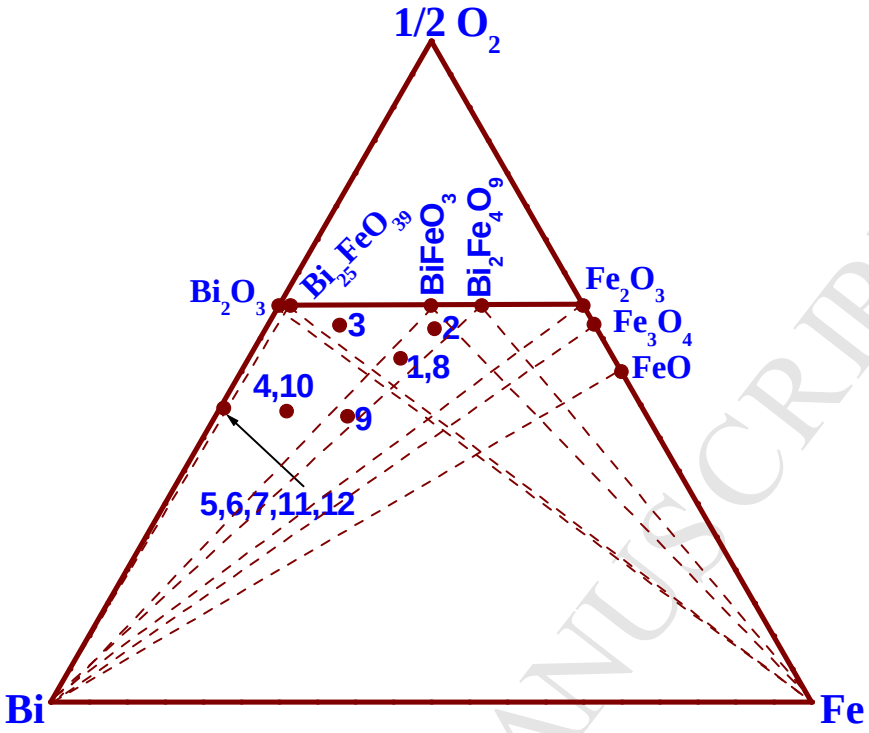

Fig. 2 **Compositions of samples taken for equilibration (1 to 12) as given in Tables 4 and 5 and possible phase fields (dotted lines) of Bi-Fe-O system**

ACCEPTED MANUSCRIPT

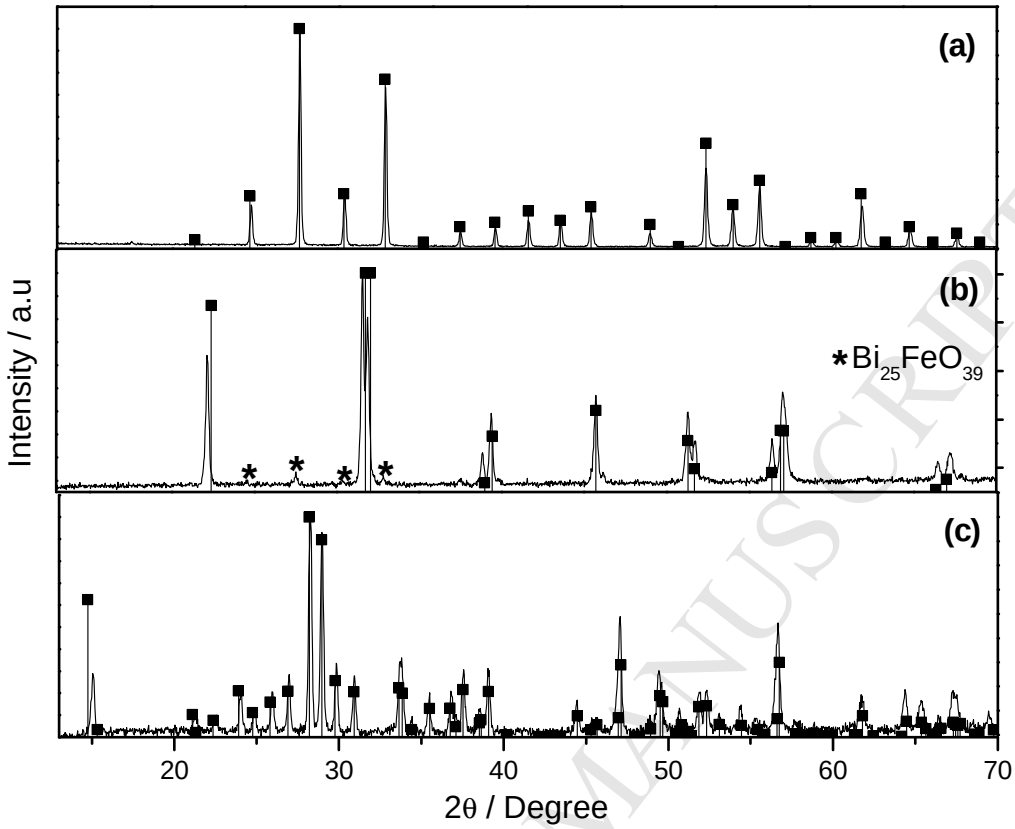

Fig. 3 XRD patterns of prepared compounds are overlapped with their respective PCPDF patterns (▮). (a) $Bi_{25}FeO_{39}$, (b) $BiFeO_3$ and (c) $Bi_2Fe_4O_9$. Small shift of XRD pattern from the PCPDF patterns is due to the instrumental shift.

ACCEPTED MANUSCRIPT

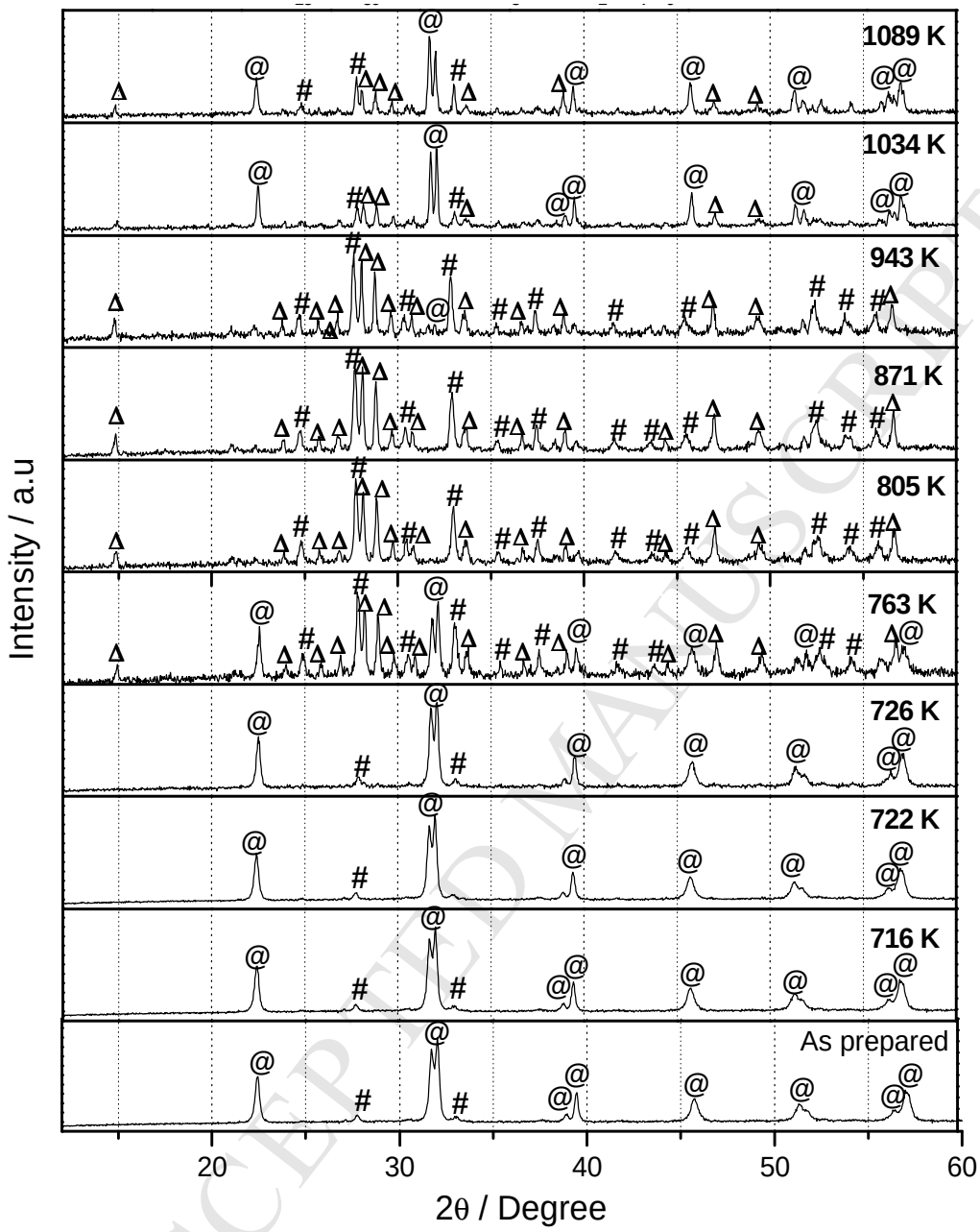

Fig. 4 **XRD patterns obtained after equilibrating $BiFeO_3$ at different temperatures in vacuum for 480 h. #: $Bi_{25}FeO_{39}$, @: $BiFeO_3$, Δ: $Bi_2Fe_4O_9$**

ACCEPTED MANUSCRIPT

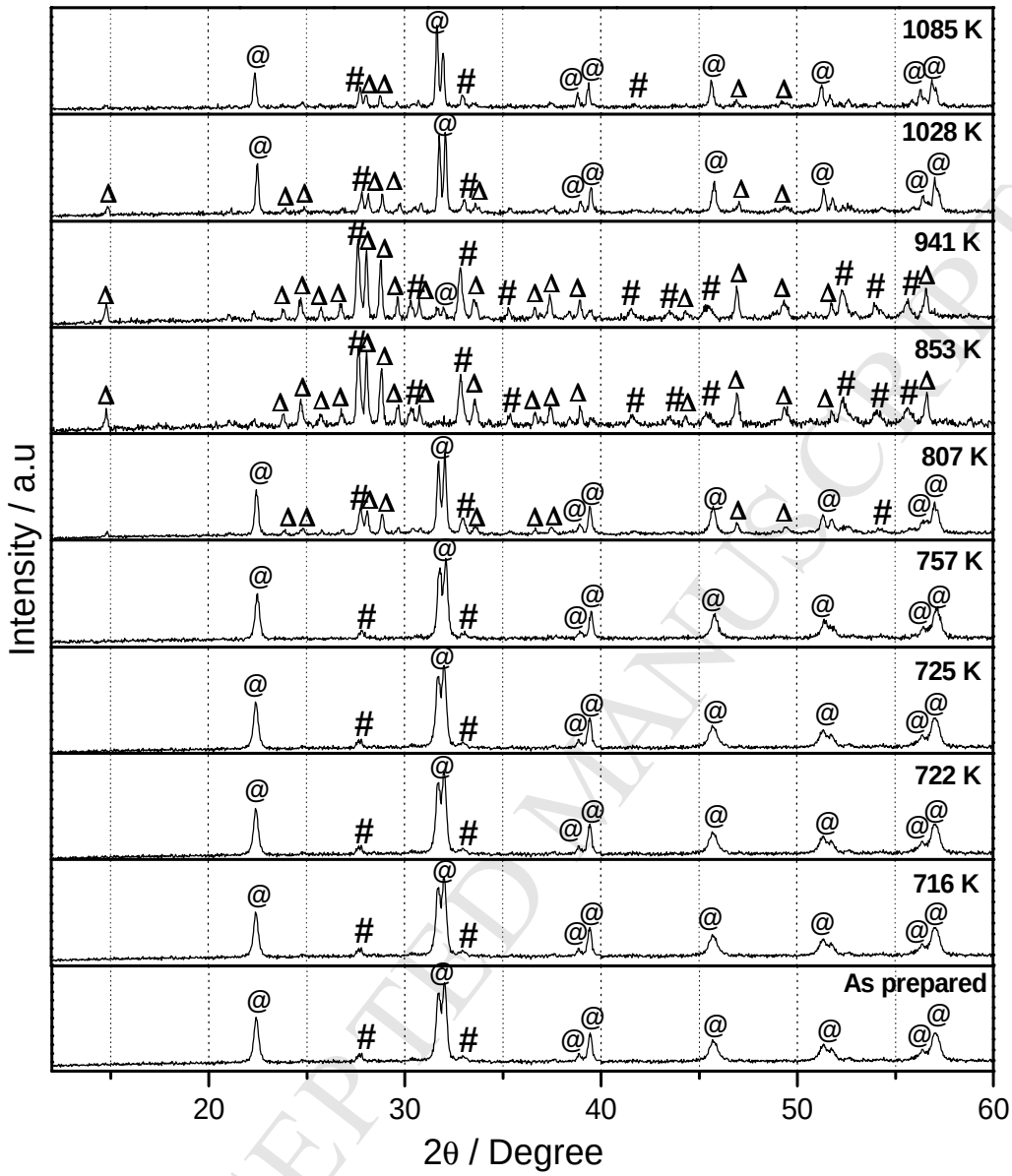

Fig. 5 **XRD patterns obtained after equilibrating $BiFeO_3$ at different temperatures in air for 480 h. #: $Bi_{25}FeO_{39}$, @: $BiFeO_3$, Δ: $Bi_2Fe_4O_9$**

ACCEPTED MANUSCRIPT

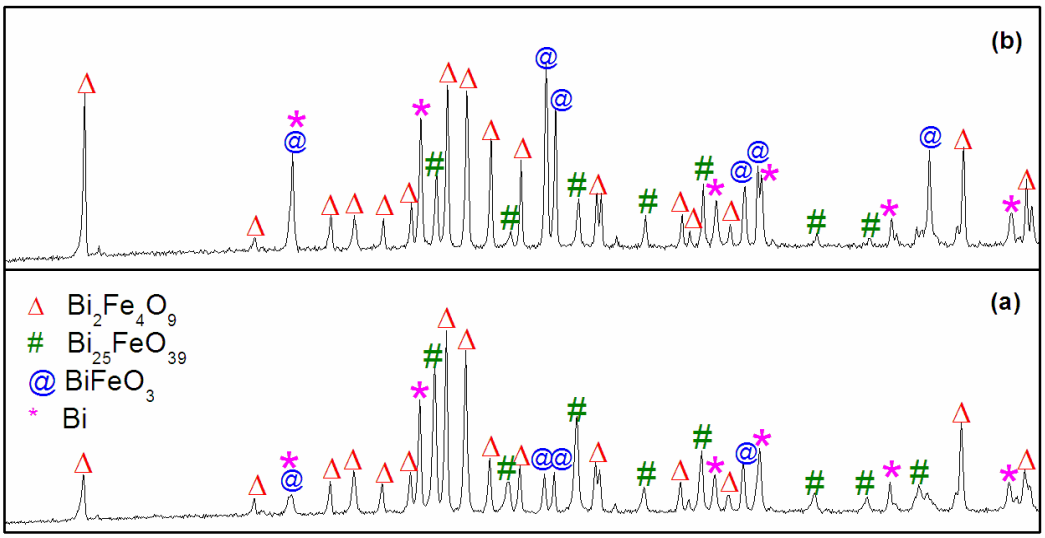

Fig. 6 **XRD patterns of the products formed after equilibration of Bi, $Bi_2Fe_4O_9$, $BiFeO_3$ mixture in liq. Bi (a) at 873 K and (b) at 1023 K for 480 h**

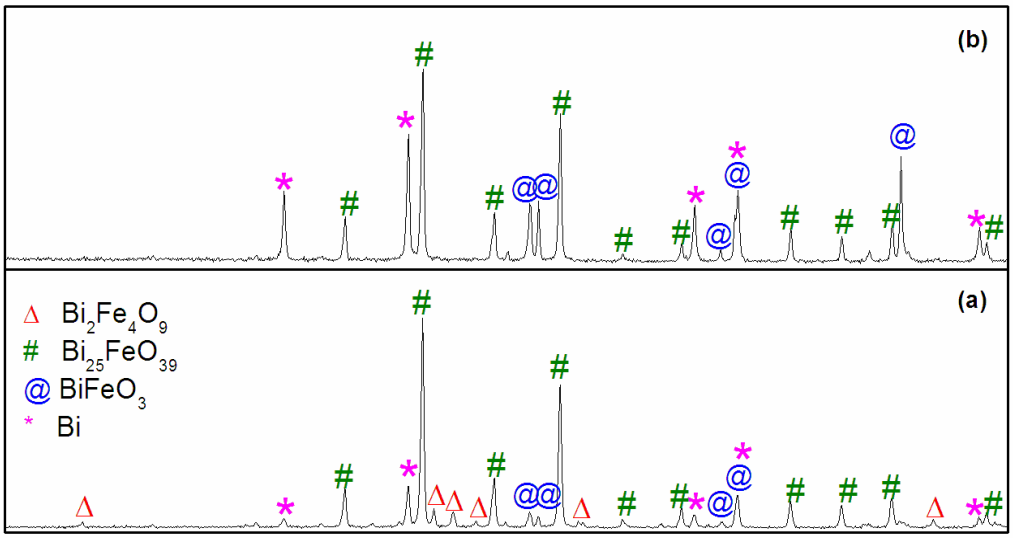

Fig. 7 **XRD patterns of the products formed after equilibration of Bi, $BiFeO_3$, $Bi_{25}FeO_{39}$ mixture in liq. Bi (a) at 873 K and (b) at 1023 K for 480 h**

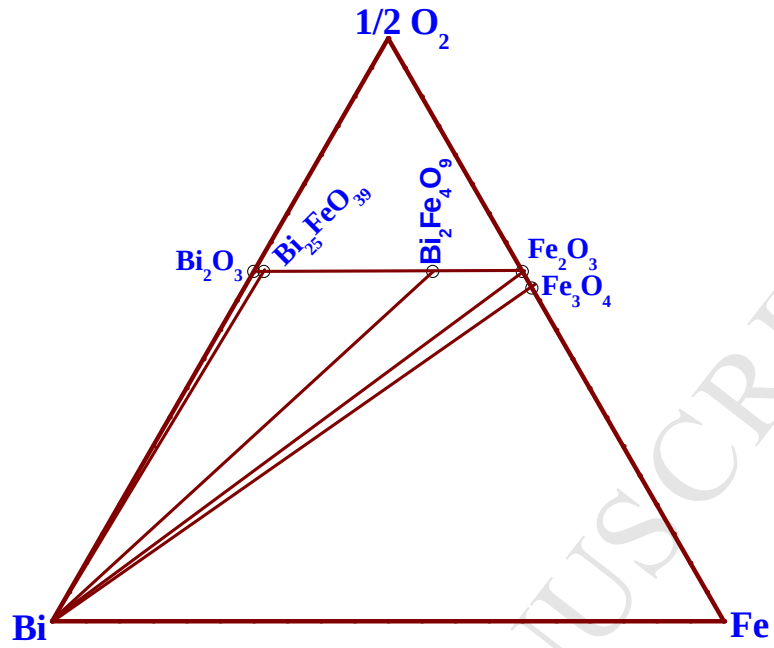

Fig. 8 **Isothermal section of the ternary phase diagram of Bi-Fe-O system at 773 K**

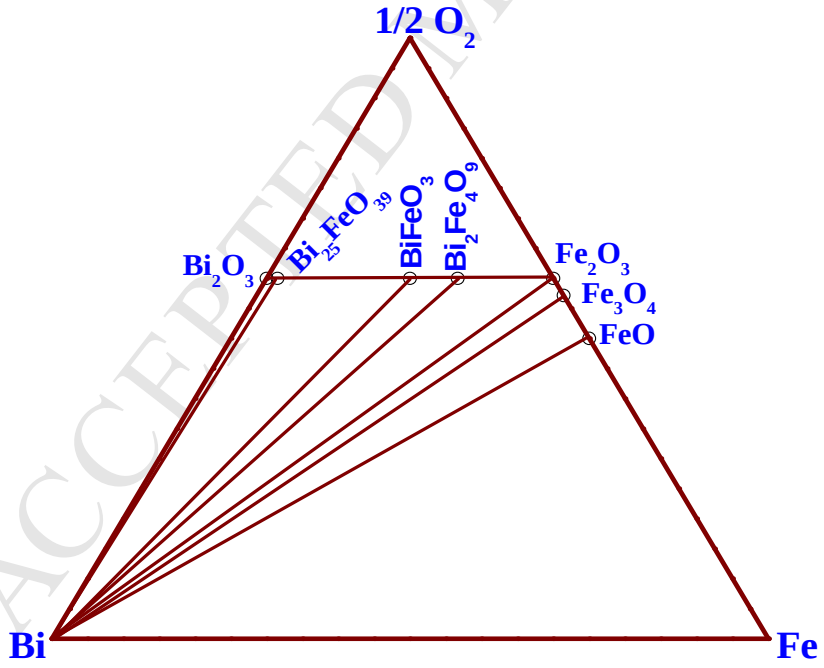

Fig. 9 **Isothermal section of the ternary phase diagram of Bi-Fe-O system at 1023 K**

ACCEPTED MANUSCRIPT

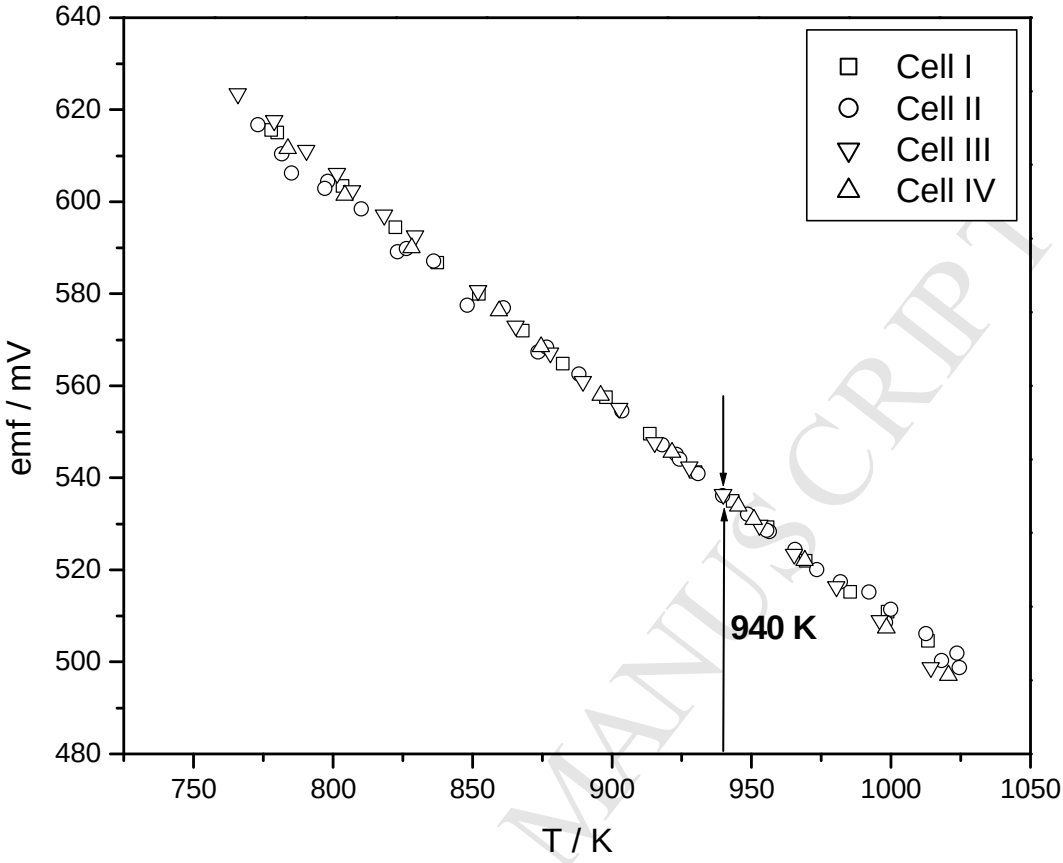

Fig. 10 Variation of emf with temperature for cells I, II, III and IV

ACCEPTED MANUSCRIPT

ACCEPTED MANUSCRIPT

Highlights

- The thermal stability of $BiFeO_3$ has been examined by different experimental techniques.
- $BiFeO_3$ is metastable at low temperatures achieves thermodynamic stability at 940 K.
- The ternary phase diagram of Bi-Fe-O system has been constructed at 773 and at 1023 K based on long term equilibration studies.

ACCEPTED MANUSCRIPT